



Research article

Platinum nanoparticles-embedded single-walled carbon nanotubes as a new carrier for curcumin delivery and investigating its anticancer effect on cell line 4T1

Ali Mohammadi^{a,b}, Fariba Bagheri^b, Yasamin Abutalebi^b, Afsoon Aghaei^c,
Hossein Danafar^{a,b,*}

^a Zanzan Pharmaceutical Nanotechnology Research Center, Zanzan University of Medical Sciences, Zanzan, Iran

^b Zanzan Pharmaceutical Biotechnology Research Center, Zanzan University of Medical Sciences, Zanzan, Iran

^c Department of Chemistry, University of Zanzan, Zanzan, Iran

ARTICLE INFO

Keywords:

Radiation therapy

Radiosensitizer

Single-walled carbon nanotubes-platinum nanoparticles -curcumin

Cancer

ABSTRACT

Cancer, a prevalent disease across various societies, presents a significant challenge in treatment research. Studies show that combination therapies are one of the methods that can help in the effective treatment of cancer. Chemotherapy and radiation therapy are among the main cancer treatments and in this project, for combined chemoradiotherapy treatment, carbon nanotubes were used as improved carriers of chemotherapy in tumors, as well as a substrate for the preparation of radiation sensitizers for local radiation therapy. Following the synthesis of CNT-Platinum-Curcumin nanoparticles (CNT-Pt-CUR), a series of analyses were conducted to verify the successful production of these nanoparticles. Techniques such as Transmission Electron Microscopy (TEM), Dynamic Light Scattering (DLS), UV-Vis spectroscopy, Fourier Transform Infrared Spectroscopy (FTIR), and X-Ray Diffraction (XRD) were employed. The characterization data revealed a spherical shape Pt nanoparticle morphology with an 8.5 nm diameter on rod-shape CNT, as observed through TEM. Furthermore, FTIR analysis confirmed the successful loaded of the drug into the nanoparticles, highlighting the potential of this approach in cancer treatment. Then, hemolysis and (3-(4,5-dimethylthiazol-2-yl)-2,5-diphenyltetrazolium bromide (MTT) tests on normal cells were used to assess the biocompatibility of CNT-Pt-CUR nanoparticles. It also explored the anticancer efficacy of these nanoparticles at varying concentrations against cancer cells, both with and without exposure to X-rays. The research confirmed the successful synthesis of these nanoparticles and demonstrated their potential impact on cell viability. Specifically, breast cancer cells exhibited heightened susceptibility to toxicity when exposed to nanoparticles and X-rays. Further analysis revealed that the toxicity of nanoparticles is dose-dependent, and modifying the surface of carbon nanotube (CNT) nanoparticles with CUR significantly reduced blood toxicity. Interestingly, nanoparticle toxicity was significantly amplified in the presence of X-rays, suggesting mechanisms such as DNA damage and increased reactive oxygen species (ROS) levels within cells.

* Corresponding author. Department of Medicinal Chemistry School of Pharmacy Zanzan University of Medical Sciences, Postal Code 45139-56184, Zanzan, Iran.

E-mail address: danafar@zums.ac.ir (H. Danafar).

<https://doi.org/10.1016/j.heliyon.2024.e33703>

Received 27 March 2024; Received in revised form 6 June 2024; Accepted 25 June 2024

Available online 26 June 2024

2405-8440/© 2024 The Authors. Published by Elsevier Ltd. This is an open access article under the CC BY-NC license (<http://creativecommons.org/licenses/by-nc/4.0/>).

1. Introduction

Cancer is one of the major causes of death globally. The most common type of cancer in women is breast cancer [1]. According to the 2020 annual report, 55.9 % of women are diagnosed with breast cancer, over the last 25 years, global trends in breast cancer incidence and mortality of 12.8 % indicate a remarkable rise worldwide [2,3]. Endocrine factors, environmental factors, and genetic factors are three important factors related to breast cancer [4]. Currently, the main methods that exist for the treatment of cancer include surgery, chemotherapy, and radiation therapy [5,6]. Each of the above methods has disadvantages that cause limitations in the effective treatment of cancer, including being invasive and the possibility of cancer recurrence in surgery, not targeting the drugs to the cancerous tissue, the problems of dissolution of some drugs, and high side effects in chemotherapy. damage to healthy cells during radiation therapy due to exposure to X-rays is one of the treatment limitations of the above methods [7]. When drug delivery systems (DDSs) are utilized during the healing process, it is possible to minimize the limitations and constraints associated with them [8]. These technologies offer focused and efficient delivery, resulting in fewer side effects and a lower risk of tumor recurrence [9,10]. Nanoparticle delivery systems including nanoparticles, hydrogels, dendrimers, micelles, and liposomes [11]. Offer a revolutionary approach to drug design and administration and change the pharmacokinetic characteristics of commonly used chemotherapeutic drugs reducing adverse effects of some otherwise very toxic chemotherapeutic drugs by enabling targeted delivery [12]. CNTs have been widely employed in previous studies [13]. The chemical and mechanical properties of CNTs make them promising candidates for drug delivery platforms. These nanostructures can be customized by incorporating biomolecules like proteins, antibodies, or DNA [14]. Carbon nanotubes (CNTs) are structures composed of carbon atoms arranged in a hexagonal pattern. These structures have a cylindrical shape with diameters that can range from 2.5 to 100 nm. The classification of these nanostructures as single-walled or multi-walled depends on the number of carbon sheets they contain. Carbon nanotubes (CNTs) have been found to be the strongest and most rigid materials in terms of tensile strength and modulus [15]. Despite their exceptional properties and numerous applications, the hydrophobic nature, toxic effects, and potential for inflammation of SWCNTs, limit their use [16]. Among parameters such as length, size, biological composition, and functionalization degree parameter, length and size parameters are important factors in CNT toxicity [17]. The toxicity of single-walled carbon nanotubes (SWCNTs) can be reduced through surface modifications [18]. PtNPs have attracted researchers' interest in various sectors, including the chemical industry, automotive, biomedical, and therapeutic fields. In the biomedical field, PtNPs have shown perfect biocompatibility, high surface/volume ratio, small size, enhanced reactivity, and electro catalytic properties. These properties make them suitable for biomedical uses, such as nanoenzymes with behaviors similar to those of superoxide dismutase and catalase. Additionally, PtNPs have optical characteristics related to surface plasmon resonance (SPR), making them potential candidates for radiotherapy agents [19]. Radiation therapy is an important component of cancer treatment, and approximately 50 % of cancer patients receive radiation therapy during their illness. The main mechanism by which radiotherapy destroys cancer is the production of reactive species (ROS) and damage to cellular components such as proteins, lipids, and DNA, which ultimately stop cell proliferation and cause necrosis or even apoptosis [20,21]. One of the most important challenges in radiation therapy is that a large percentage of patients show resistance to RT. Ionizing radiation affects both healthy tissues and solid tumors. Since the surrounding tissue is also affected by radiation, increasing the radiation dose often results in damage to normal tissues [22]. That is why radiotherapy requires improvements in radiation delivery techniques to reduce damage to surrounding tissues. Radiosensitizers are a suitable solution to overcome this problem. Radiosensitizers are adjunctive treatments that make tumor cells more susceptible to radiation. They are designed to improve the killing of tumor cells while having much less impact on normal tissues. Platinum nanoparticles can be mentioned as one of the radiosensitizers [23]. CUR, a natural polyphenol, is the active ingredient found in turmeric. It has been historically utilized as a medicinal plant due to its antioxidant, anti-inflammatory, anti-mutagenic, antimicrobial, and anticancer properties [24], anti-mutagenic, antimicrobial [25,26], and anticancer properties. In terms of solubility, CUR is soluble in alkaline or highly acidic solvents [27]. Curcuminoid compound with a predominant keto form in acidic or neutral solutions, while the enol form is dominant in alkaline solutions and exhibits good chelating properties for metal ions [28]. It has been demonstrated over the past 50 years that majority of the benefits of turmeric are mainly due to CUR, which may have impacts on diabetes, allergies, arthritis, Alzheimer's disease [29], and other chronic diseases [30]. In the current investigation, it was aimed at using platinum nanoparticles as a radiosensitizer to increase the intensity of radiation in cancer cells. We synthesized these nanoparticles on carbon nanotubes and used this carrier for the delivery of CUR for combined chemoradiotherapy treatment.

2. Material and methods

2.1. Materials

Curcumin was provided from the Merck (Germany). The 4T1 cell line and the HFF-2 cell line were obtained from the Pasteur Institute (Iran). MTT was procured from Sigma (USA), Fluka (St. Gallen, Switzerland). Ethanol was from Kimia alcohol (Iran). Hexachloroplatinic(IV) acid hexahydrate (~40 % Pt) and Dimethylsulfoxide (DMSO) were obtain from the Merck (Germany). Growth medium, DMEM, Fetal Bovine Serum, Penicillin, Streptomycin, and phosphoric acid were from Gibco (Germany). All other chemicals were analytical-grade and commercial products.

2.1.1. Synthesis method of platinum-modified CNTs

For the synthesis and purification of Single-Walled Carbon Nanotubes (SWCNTs) functionalized with Fe–Mo catalyst, we adopted a methodology previously reported [31]. In order to synthesize SWCNTs-Pt, 11.75 μL of $\text{H}_2\text{PtCl}_6 \cdot 6\text{H}_2\text{O}$ (1 M) solution was added in drops to a solution of 4.7 mg SWCNTs, followed by the addition of freshly prepared NaBH_4 solution with a concentration of 0.21 mg/mL

dropwise to the reaction. The mixture was stirred at room temperature for 12 h, followed by purified through dialysis for 48 h.

2.1.2. Curcumin loading on CNT-Pt

4 mg of CUR was dissolved in 1.25 mL of acetone. This solution was then gradually added into a 20 mg aqueous CNT-Pt. The mixture was stirred at room temperature using a magnetic stirrer for a duration of 24 h. Following this, to purify CNT-Pt-CUR, due to CUR's low solubility in water, a centrifugation process was employed at 14,000 rpm using 30 % ethanol. This procedure was repeated multiple times.

2.1.3. Determining the structure, physical and chemical properties

Various techniques, such as TEM, DLS, UV-vis, FTIR, all of them were conducted according to the previous study [31].

2.1.4. Study of the effect of curcumin diffusion under different pH conditions

The synthesized nanosystem was dispersed three times in 1.5 mL of phosphate-ethanol buffer at pH 7.4, simulating physiological conditions, at pH 4.7, mimicking the acidic environment of tumors, each time incorporating 4 mg of the nanosystem. Following dispersion, the nanosystems were placed in dialysis bags and submerged in 15 mL of phosphate-ethanol buffer within containers. These containers were then incubated at 37 °C in a shaker. At various intervals, samples were extracted and analyzed for absorbance at 430 nm using a UV-Vis. The absorbance data were utilized to determine the concentration of the released drug. Finally, the results of the drug release measurements were plotted as the concentration of the released drug over a period of 50 h the evaluation of the drug measurement method was conducted based on linearity, accuracy, recovery, limit of detection, and limit of quantification, adhering to the standards outlined in the United States Pharmacopoeia.

2.1.5. Cell culture

The 4T1 cells, sourced from the Pasture Institute in Tehran, Iran, were employed in this research. Initially, the cells were cultivated in Dulbecco's Modified Eagle's Medium (DMEM), which is supplemented with 10 % Fetal Bovine Serum (FBS) and 1 % Penicillin/Streptomycin (Pen/Strep) from Sigma-Aldrich. The culture was maintained at 37 °C, with 5 % CO₂, for 24 h until the cells achieved 70–80 % confluence, then cell passage was performed. After removing the culture medium from the flask, the cells were washed twice with 1 mL of Phosphate Buffered Saline (PBS). To facilitate detachment, 1 mL of a 25 % trypsin-EDTA solution was added to the flask and incubated for approximately 4-3 min. To neutralize the trypsin, 3 mL of culture medium enriched with serum was added, after which the mixture was transferred to a Falcon tube and centrifuged at 1700 rpm for 7 min. The resulting cell pellet was then dispersed, and the suspension was equally distributed between two new flasks before returned to the incubator.

2.2. Cell viability study

4T1 cells were seeded at a density of 7000 cells per well in a 96-well plate. To assess the cytotoxic effects of nanoparticles after incubation with 4T1, for 24 h on these cells, the MTT assay, the 3-(4,5-dimethylthiazol-2-yl)-2,5-diphenyltetrazolium bromide, was employed. The control groups, 4T1 cells left untreated. The samples were incubated with MTT solution (100 µL, 1 in DMEM media) for 4 h. After 4 h incubation repeatedly, 100 µL of DMSO was added to each well, and their absorbance at a specific wavelength of 570 nm was measured. the procedure was repeated at least five times.

2.3. Hemolysis assay

In summary, 200 µL of human red blood cells were mixed with 800 µL of a solution containing different concentrations of samples. The samples were shaken in an incubator shaker at a temperature of 37 °C for 4 h. Deionized water was used as a positive control, while a PBS solution was used as a negative control. After the incubation, the samples were centrifuged at 1300 rpm for 15 min. Subsequently, the absorbance of the resulting solution was measured at 540 nm. Finally, the percentage of hemolysis in the samples was calculated using the given equations.

$$\text{Hemolysis(\%)} = \frac{A_{\text{sample}} - A_{\text{negative}}}{A_{\text{positive}} - A_{\text{negative}}} \times 100$$

2.4. Determination of toxicity on healthy cells

The cytotoxicity of the synthesized nanoscale system was assessed on the HFF-2 cell line using an MTT assay. Cells were exposed to varying concentrations, with each concentration tested in 5 repetitions.

2.4.1. Therapeutic effects externally

Anti-cancer nanoparticles' therapeutic effects on 4T1 cancer cells were evaluated with and without X-ray radiation using the MTT assay. After transferring the cells to two 96-well plates, the cells were treated with different groups and concentrations. After 6 h incubation, the culture medium was removed and the cells were washed twice with PBS. Then, fresh culture medium was added to each well. In continuation, a plate was subjected to X-ray radiation of 6 MeV using the PRIMUS linear accelerator from Siemens, located in the radiotherapy department of Valiasr Hospital in Zanjan, Iran. The exposure consisted of a dose of 6 Gy over 120 s for the cells. The

incubation continued for another 24 h. To obtain cell viability, MTT reagent at a concentration of 10 μL with a concentration of 3 mg/mL was added to each well. After 4 h incubation, 100 μL of DMSO was added to each well, and the absorbance of each well was read at a wavelength of 570 nm. Finally, the percentage of cell viability was calculated by determining the absorbance ratio in the treated group cells compared to the control group. Each concentration was tested in sets of 5 repetitions.

3. Results

TEM imaging was used to investigate the size and morphology of the CNT-Pt-CUR nanoparticles. The images confirmed the successful production of Pt nanoparticles with an average diameter of 8.53 nm on the CNT surface. Additionally, Fig. 1 indicated that the CNT diameter was 50 nm.

3.1. Investigation of FT-IR spectra

FT-IR spectra of CUR, single-walled carbon nanotubes, and single-walled carbon nanotubes containing CUR demonstrated. The empty CUR spectrum displayed a distinct peak at 3442 cm^{-1} , indicating the vibrations of O-H bonds. This peak in the CNT-Pt-CUR spectrum became narrower compared to empty CUR and shifts to 3438 cm^{-1} , indicating the formation of hydrogen bonds between CUR and CNT-Pt. In the CNT-Pt-CUR spectrum, peaks at 1574 cm^{-1} and 1420 cm^{-1} , are observed similar to those in CUR and single-walled carbon nanotubes spectra. These peaks indicated that the presence of aromatic carbon-carbon double bonds ($\text{C}=\text{C}$). Furthermore, a peak at 1640 cm^{-1} is noted, which corresponds to the vibrations of $\text{C}=\text{O}$, according to Fig. 2.

3.1.1. UV-vis spectrophotometer

To verify the successful loading of CUR onto the CNT-PT nanocarrier, a UV-Vis spectroscopy analysis was conducted (see Fig. 3). This analysis revealed the characteristic absorption peaks of CUR at 430 nm and CNT-PT nanocarrier at 264 nm. Interestingly, a slight red shift of approximately 2 nm was observed in the final nanosystem, indicating the interaction between CUR and the nanocarrier.

3.1.2. Analysis of the X-ray scattering pattern of synthesized carbon nanotubes

The XRD pattern of the prepared CNT-Pt is depicted in Fig. 4. According to the results, the obtained XRD pattern showed the peaks of both constituents of the sample (i.e., CNT and Platinum). In this regard, three XRD peaks at approximately 39.7° , 46.2° , and 66.8° were observed for Platine constitute of the samples that correspond to its (111), (200), and (220), crystallographic planes, respectively. The CNT parts of the sample also revealed three corresponding peaks at 25° , 46.2° , and 55.9° , which attributed to its (002), (100), and (004) crystal planes. The presence of the XRD peaks of both CNT and Platine in the obtained XRD pattern indicates successful synthesizing of CNT-Platine nanoparticles. The diffraction peak observed at around 25.1° corresponds with the carbon (0 0 2) reflection of the graphitic planes of the SWCNT (JCPDS card no. 75-1621). The peaks appearing at diffraction angles of 39.8° , 46.2° and 67.7° (JCPDS-ICDD, Card No. 04-802) are corresponding to the face-centered cubic crystal (fcc) planes of (1 1 1), (2 0 0), (2 2 0), (3 1 1), (222) respectively [32].

3.1.3. Zeta potential distribution

The average values of the zeta potential of CNT-Pt -11eV and CNT-Pt-CUR -14eV were observed (Fig. 5). Regarding the impact of surface charge on blood circulation and stability, it is expected that CUR loaded with a decrease in surface charge and non-identification particles by RES will enhance blood circulation in the body.

3.1.4. Drug-loading content

The drug loading was calculated using the given equation, resulting in a CUR loading amount of 27.14 %, with 90 % yield of nanoparticles.

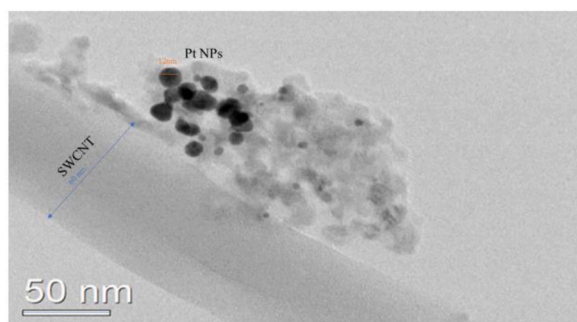


Fig. 1. TEM micrographs of CNT-Pt-CUR nanoparticles at various scale bars.

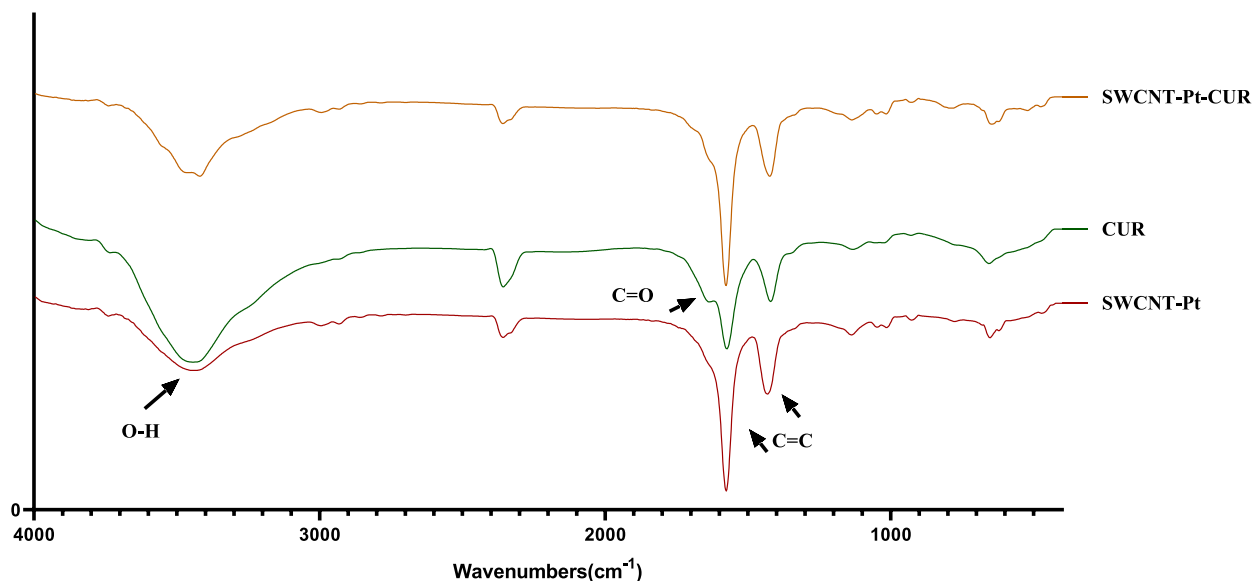


Fig. 2. FT-IR spectrum related to CUR and SWCNT-Pt-CUR and SWCNT-Pt.

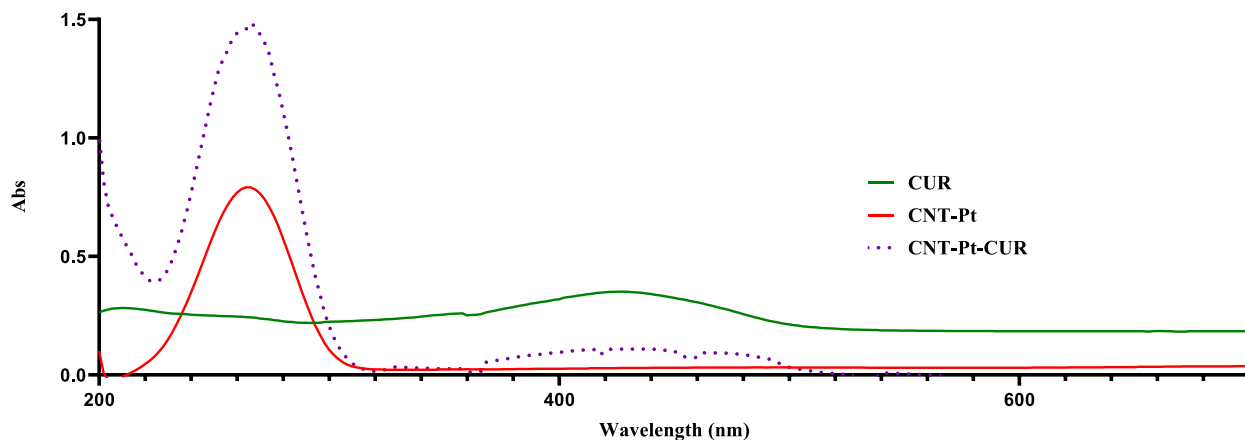


Fig. 3. The UV-Vis spectrum of the samples CUR, CNT-Pt, and CNT-Pt-CUR.

$$\text{drug loading content(\%)} = \frac{\text{weight of the drug in nanoparticles}}{\text{weight of the nanoparticles with drug}} \times 100$$

3.2. Drug release study

The study examined drug release in a phosphate-ethanol buffer under two distinct pH levels: 7.4 and 4.7. The pH 7.4 was chosen to mimic physiological body conditions, while the pH 4.7 was selected to simulate tumor conditions. The release of CUR in an acidic environment was 79 %, whereas in a physiological environment, it was only 39 %. This indicates that the release of CUR from CNT-Pt-CUR is pH-sensitive, with a higher release rate in acidic conditions compared to physiological one's Fig. 6.

3.3. Determining the damages inflicted on red blood cells (hemolysis)

The blood toxicity of the synthesized Nanosystem of CUR with concentrations of 7.5, 15, 30, and 60 $\mu\text{g/mL}$, CNT-Pt with concentrations of 50, 100, 200, and 400 $\mu\text{g/mL}$, and SWCNT-Pt- CUR with concentrations of 50, 100, 200, and 400 $\mu\text{g/mL}$ were investigated. As shown in Fig. 7 only CNT-Pt exhibited toxicity at concentrations of 200 and 400 $\mu\text{g/mL}$. Moreover, the data indicated that the toxicity resulting from loading the CUR drug on CNT-Pt has decreased, which this decrease in toxicity can be indicative of successful surface coverage of CNT-Pt with the CUR drug and the modification of the surface of the prepared nanosystem. The results of the hemolysis test for the other compounds and concentrations were calculated to be less than 5 %, indicating the safety of the Nano

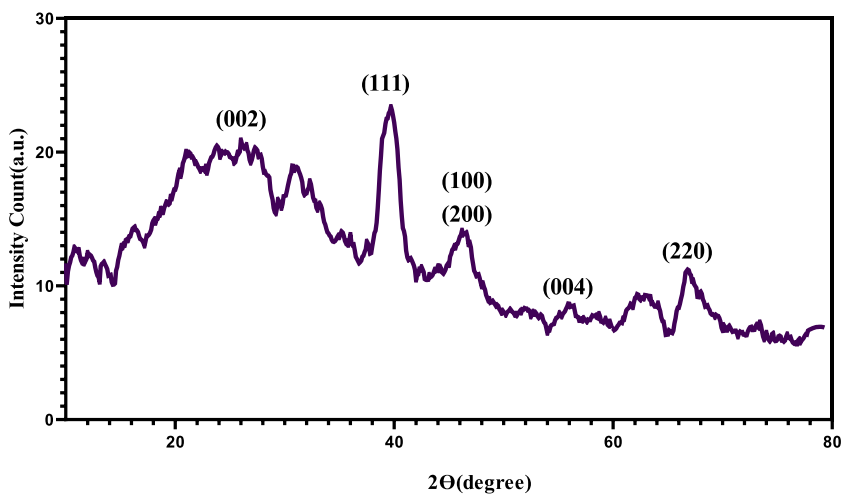


Fig. 4. The XRD spectrum is related to single-walled carbon nanotubes (SWCNT-Pt).

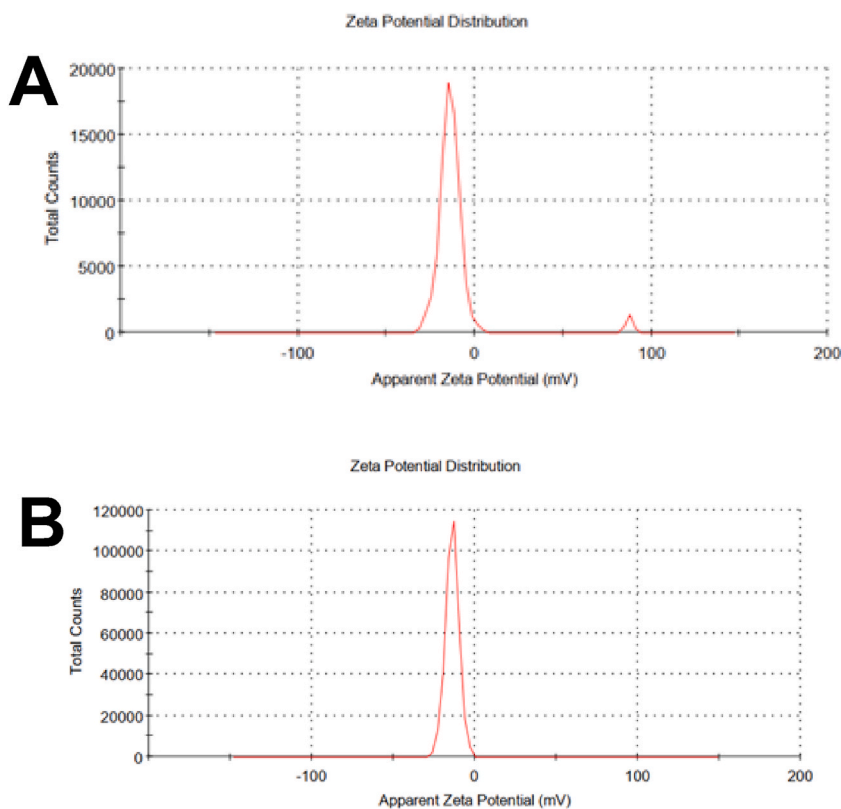


Fig. 5. Zeta potential distribution (A CNT-Pt and B CNT-Pt-CUR).

formulation.

3.4. Investigation of the toxicity effect on HFF-2 cell line

Before investigating the anticancer activity of the synthesized compound, the toxicity of nanoparticles on healthy embryonic fibroblast cells was examined. HFF2 cells were treated with different concentrations of nanoparticles, and cell viability was determined using the MTT assay. The results were presented in Fig. 8 indicating that the toxicity of nanoparticles increased with an increase in the concentration of SWCNT-Pt. However, cell viability increased when loaded with CUR, which could be attributed to surface chemistry.

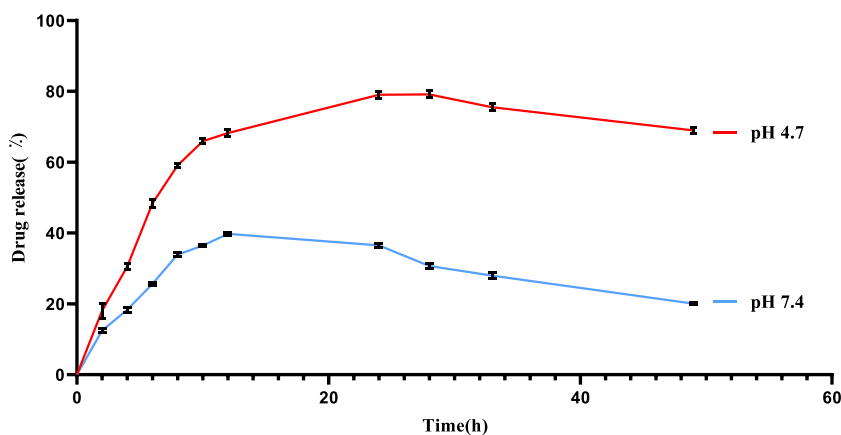


Fig. 6. The CUR release profile of loaded CNT-Pt in pH 7.4 and 4.7. Drug release from loaded CNT-Pt in pH 7.4 was remarkably lower than that of pH 4.7.

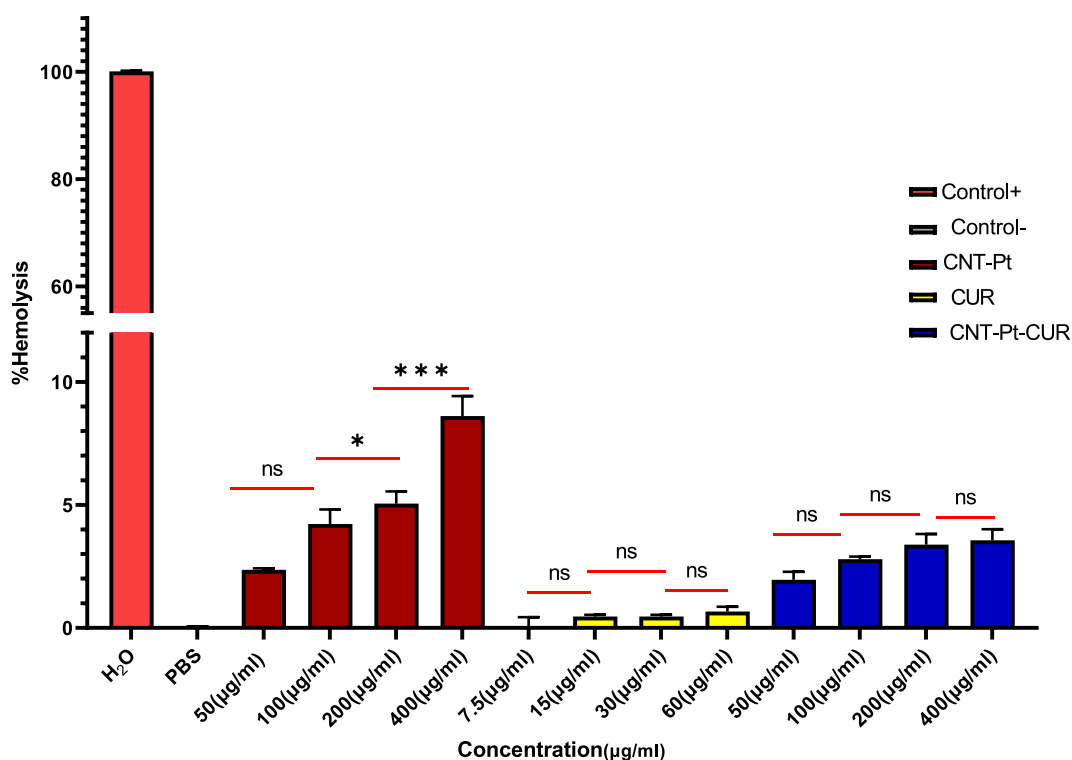


Fig. 7. Examining blood toxicity of CUR nanosystems, including CNT-Pt and CNT-Pt- CUR, at various concentrations, (the assays were performed and reported as the mean \pm SD, * $p < 0.05$; *** $p < 0.001$, ns: non-significant).

The control group exhibited no significant variation with CUR at concentrations of 4, 15, and 20 $\mu\text{g/mL}$, which could be due to the low potential of CUR compared to other anticancer drugs, because of low solubility or low penetration ability into cells. Nevertheless, according to the data, the investigation of the toxicity effect on the HFF-2 cell line showed no toxicity at CUR concentrations up to 20 $\mu\text{g/mL}$.

3.4.1. Therapeutic effects on cancer cells with or without X-ray radiation

Cells exposed to X-ray radiation exhibit a survival rate of approximately 81%. Additionally, cells exposed to X-ray radiation in the presence of nanoparticles exhibit significantly decrease survival rates, which clearly depend on the concentration. Cellular survival in the presence of nanoparticles at concentrations of 25 $\mu\text{g/mL}$, 75 $\mu\text{g/mL}$, and 100 $\mu\text{g/mL}$, and under X-ray radiation (Gy6), is lower compared to the non-irradiated group and indicates higher cellular cytotoxicity. The results indicated that the presence of CNT-Pt

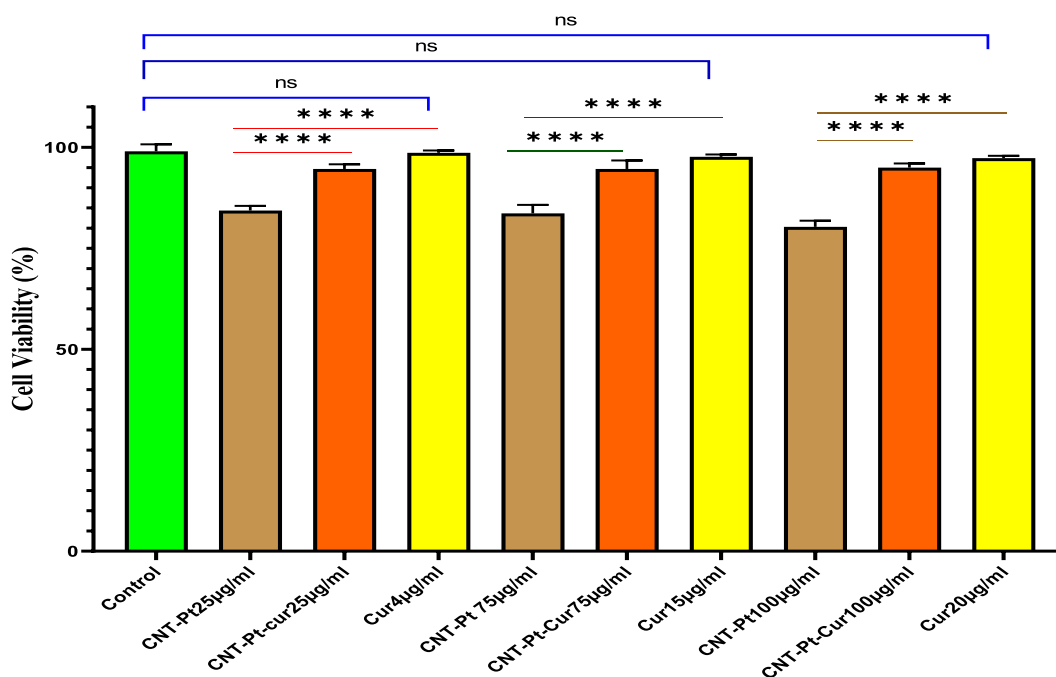


Fig. 8. The impact of nanoparticles on healthy embryonic fibroblast cells, specifically HFF2 cells, was assessed through varying concentrations of nanoparticles. Results were reported as mean \pm SD, with 'ns' indicating non-significant findings.

nanoparticles enhances the effect of radiotherapy. MTT assays revealed that the combination of X-ray radiation with sensitizing nanoparticles, led to greater cell damage, which can be attributed to the increased production of reactive oxygen species in the presence of platinum nanoparticles Fig. 9.

4. Discussion

This study investigates the use of CNT-Pt nanoparticles loaded with CUR as a radiosensitizer. Initially, the nanoparticles were synthesized and characterized. Subsequently, the release of CUR in a tumor-simulating medium at physiological pH was examined. The efficacy of the synthetic nanosystem as a radiosensitizer on cancer cells was evaluated *in vitro*. Over the past few decades, nanomaterial-based sensitizers containing high atomic number atoms have attracted considerable interest, particularly in cancer therapy [33,34]. These nanosystems, including those coated with suitable materials, can exploit the Enhanced Permeability and Retention (EPR) effect to deliver nanoparticles to tumor regions [35]. Materials rich in high atomic number elements, such as gold, silver, platinum, and copper, can concentrate ionizing radiation in the target tissue, generating primary and secondary electrons under X-ray radiation. This process leads to an increase in reactive oxygen species and cellular damage [36]. In this study, carbon nanotubes were prepared according to the method described, followed by the addition of platinum and then CUR, which was carefully loaded onto the nanocarrier. The size of drug delivery particles significantly influences their ability to undergo endocytosis by epithelial and endothelial cells and their longevity during systemic circulation. To evade detection and destruction by the immune system, these nanoparticles must be appropriately small [37]. The obtained nanoparticles are suitable for prolonging blood circulation as well as can penetrate tissues and cells because of they are smaller than the physiological pores and fenestrations of the body (intestinal lumen, endothelial connections, and tumors). Single-wall carbon nanotubes imbedded with platinum nanoparticles with a size of 8.5 nm and a surface charge of -14 eV demonstrates the significant potential of the designed Nanotechnology in drug delivery and the high capability of blood circulation in the designed system. Therefore, it may be claimed that CUR-loaded carbon nanotubes were fabricated properly with a proper size and good morphology. The analysis of the XRD graph reveals that the synthesized nanoparticles' XRD pattern aligns with the standard pattern, confirming the successful production of SWCNT-Pt [38]. Furthermore, UV-Vis and FTIR analyses were employed to modify the surface of the prepared particles and investigate molecular interactions. These analyses confirm the successful incorporation of the drug onto the nanocarrier. The drug release experiment revealed that the release of the drug is pH-dependent, with higher release rates observed at acidic pH levels, mirroring the conditions of a tumor tissue simulator. Approximately 79% of CUR was released during the experiment. To evaluate the blood compatibility of the formulation, a hemolysis test was conducted. The findings of the cytotoxicity of CNT studies on the HFF-2 cell line confirmed the results of the hemolysis experiments, which show that the toxicity of the prepared nanosystem is dose-dependent and that its surface toxicity can be reduced through surface modification with drug loading. A related study showed that CUR coating significantly reduced the inflammatory and cell death-inducing potential in MWCNT [39]. Nanoparticles exhibit minimal toxicity towards 4T1 cancer cells on their own, and X-ray radiation at the applied dose also did not show high toxicity. However, when combined, radiotherapy and nanoparticles significantly

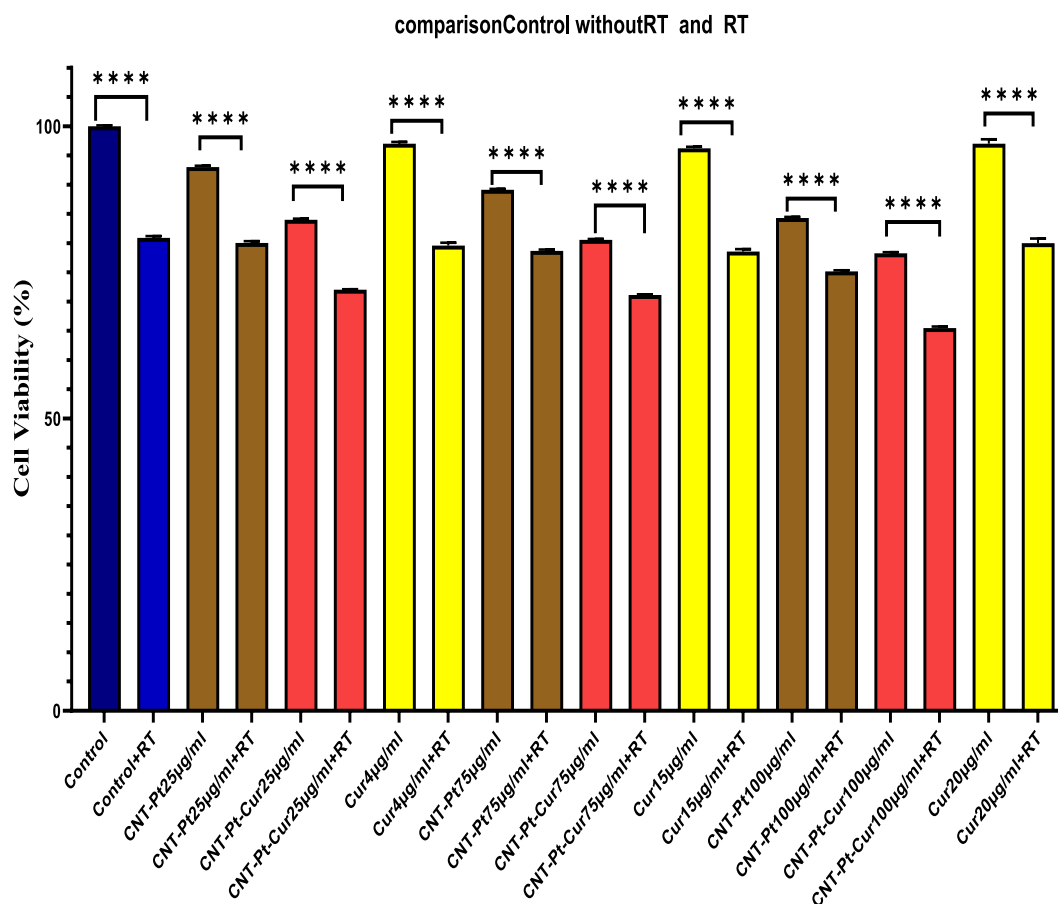


Fig. 9. Sensitivity of radiation to CNT-Pt-CUR nanoparticles is indicated by the following symbols: ns, *, **, ***, and **** respectively indicate no significant difference, significant difference with $05/0 p =$, significant difference with $p < 0.01$, significant difference with $p < 0.001$, and significant difference with $p < 0.0001$.

enhance cytotoxicity or therapeutic efficacy across all tested concentrations. Investigations by Abed and colleagues revealed that porous platinum nanoparticles could induce DNA damage, generate ROS, and cause substantial cell cycle arrest [40]. Furthermore, the study demonstrated that X-ray radiation, when paired with sensitizing nanoparticles, leads to increased cellular damage. This enhanced effect is attributed to the generation of secondary electron cascades and an increase in intracellular ROS by platinum nanoparticle sensitizers in the presence of X-ray radiation [41].

5. Conclusion

The data obtained from this project showed the successful synthesis of the multipurpose nanosystem CNT-Pt with chemotherapy and radiation therapy capabilities, and the most important limitation of CNTs, i.e. their toxicity, was significantly reduced by surface modification through coating with CUR. The synthesis of CNT-Pt-CUR, is validated through several techniques such as TEM, XRD, UV-Vis, DLS and FTIR. The characterization data revealed a spherical shape Pt nanoparticle morphology with an 8.5 nm diameter on rod-shape CNT, as observed through TEM. The successful loading of curcumin onto CNT-Pt-CUR nanoparticles is confirmed by FTIR and UV-vis spectroscopy. Drug loading of CUR is 27.14 %, with 90 % yield of nanoparticles. The drug release experiment revealed that the release of the drug is pH-dependent, with higher release rates observed at acidic pH. Finally, the anticancer effect of the CNT-Pt-CUR nanoparticles is evaluated on 4T1 cancer cells. The lowest survival rate of cancer cells with chemotherapy and radiation therapy indicates the significantly enhance cytotoxicity or therapeutic efficacy. These results provide guidance towards a more successful and comprehensive treatment of breast cancer in the future.

Ethics approval consent to participate

All the experiments were compliant with research ethic committee guidelines and approved by the animal care ethics committee of the Zanzan University of Medical Science (ethical code: IR. ZUMS. BLC.1401.011)

Consent for publication

No applicable.

Availability of data and materials

The dataset used and/or analyzed during the current study available from the corresponding author on reasonable request.

Funding

This work was supported by the Deputy of Research of Zanjan University of Medical Sciences [A-12-430-63, ethical code: IR. ZUMS. BLC.1401.011].

CRediT authorship contribution statement

Ali Mohammadi: Formal analysis. **Fariba Bagheri:** Methodology. **Yasamin Abutalebi:** Project administration. **Afsoon Aghaei:** Methodology. **Hossein Danafar:** Supervision.

Declaration of competing interest

The authors declare that they have no known competing financial interests or personal relationships that could have appeared to influence the work reported in this paper.

Acknowledgements

This work was supported by the Deputy of Research of Zanjan University of Medical Sciences [A-12-430-63, ethical code: IR. ZUMS. BLC.1401.011].

References

- [1] Q. Chen, et al., Novel targeted pH-responsive drug delivery systems based on PEGMA-modified bimetallic Prussian blue analogs for breast cancer chemotherapy, *RSC Adv.* 13 (3) (2023) 1684–1700.
- [2] R. Fan, et al., Application of aptamer-drug delivery system in the therapy of breast cancer, *Biomed. Pharmacother.* 161 (2023) 114444.
- [3] J. Nel, et al., Functionalized liposomes for targeted breast cancer drug delivery, *Bioact. Mater.* 24 (2023) 401–437.
- [4] G.M. Calaf, et al., Endocrine disruptors from the environment affecting breast cancer, *Oncol. Lett.* 20 (1) (2020) 19–32.
- [5] O. Mitxelena-Iribarren, et al., Drug-loaded PCL electrospun nanofibers as anti-pancreatic cancer drug delivery systems, *Polym. Bull.* 80 (7) (2023) 7763–7778.
- [6] S.M. Amini, et al., Gold cluster encapsulated liposomes: theranostic agent with stimulus triggered release capability, *Med. Oncol.* 40 (5) (2023) 126.
- [7] S.M. Amini, Plasmonic hyperthermia or radiofrequency electric field hyperthermia of cancerous cells through green-synthesized curcumin-coated gold nanoparticles, *Laser Med. Sci.* 37 (2) (2022) 1333–1341.
- [8] S. Adepu, S. Ramakrishna, Controlled drug delivery systems: current status and future directions, *Molecules* 26 (19) (2021) 5905.
- [9] Sareh Mosleh-Shirazi, Seyed Reza Kasaei, Fatemehsadat Dehghani, Hesam Kamyab, Irina Kirpichnikova, Shreeshivadasan Chelliapan, Tahereh Firuzyar, Mohammadreza Akhtari, Mohammad Amani Ali, Investigation through the anticancer properties of green synthesized spinel ferrite nanoparticles in present and absent of laser photothermal effect, *Ceram. Int.* 49 (2023) 11293–1130110.
- [10] L. Shabani, S.R. Kasaei, S. Chelliapan, et al., An investigation into green synthesis of Ru template gold nanoparticles and the in vitro photothermal effect on the MCF-7 human breast cancer cell line, *Appl. Phys. A* 129 (2023) 564.
- [11] S. Yazdani, et al., Design of double functionalized carbon nanotube for amphotericin B and genetic material delivery, *Sci. Rep.* 12 (1) (2022) 21114.
- [12] X. Kong, et al., Nanoparticle drug delivery systems and their applications as targeted therapies for triple negative breast cancer, *Prog. Mater. Sci.* (2023) 101070.
- [13] X. Zhang, et al., Preparation of carbon nanotubes and polyhedral oligomeric-reinforced molecularly imprinted polymer composites for drug delivery of gallic acid, *Int. J. Pharm.* 615 (2022) 121476.
- [14] S.-R. Yan, et al., Rheological behavior of hybrid MWCNTs-TiO₂/EG nanofluid: a comprehensive modeling and experimental study, *J. Mol. Liq.* 308 (2020) 113058.
- [15] S. Li, et al., The molecular dynamics study of vacancy defect influence on carbon nanotube performance as drug delivery system, *Eng. Anal. Bound. Elem.* 143 (2022) 109–123.
- [16] T. Hemraj-Benny, L. Pimentel, G. Emeran, Formation of single-walled carbon nanotube-ruthenium nanoparticles in ethanol upon microwave radiation, *Inorg. Chem. Commun.* 112 (2020) 107707.
- [17] B. Dinc, E. Sen, Toxicity of short multi-walled carbon nanotubes in *Caenorhabditis elegans*, *Fullerenes, Nanotub. Carbon Nanostruct.* 30 (6) (2022) 646–656.
- [18] V. Vijayalakshmi, B. Sadanandan, A.V. Raghunath, Single walled carbon nanotubes in high concentrations is cytotoxic to the human neuronal cell LN18, *Results in Chemistry* 4 (2022) 100484.
- [19] C. Zhang, et al., Platinum-based drugs for cancer therapy and anti-tumor strategies, *Theranostics* 12 (5) (2022) 2115.
- [20] F. Busato, B.E. Khouzai, M. Mognato, Biological mechanisms to reduce radioresistance and increase the efficacy of radiotherapy: state of the art, *Int. J. Mol. Sci.* 23 (18) (2022) 10211.
- [21] A. Neshastehriz, et al., In-vitro investigation of green synthesized gold nanoparticle's role in combined photodynamic and radiation therapy of cancerous cells, *Adv. Nat. Sci. Nanosci. Nanotechnol.* 11 (4) (2020) 045006.
- [22] S. Nisar, et al., Natural products as chemo-radiation therapy sensitizers in cancers, *Biomed. Pharmacother.* 154 (2022) 113610.
- [23] Y. Kitayama, et al., In vivo stealthified molecularly imprinted polymer nanogels incorporated with gold nanoparticles for radiation therapy, *J. Mater. Chem. B* 10 (35) (2022) 6784–6791.
- [24] L. Yadav, Golden spice turmeric and its health benefits, in: *Ginger-Cultivation and Use*, IntechOpen, 2022.
- [25] R.C. Reddy, et al., Curcumin for malaria therapy, *Biochem. Biophys. Res. Commun.* 326 (2) (2005) 472–474.
- [26] S.M. Amini, et al., Curcumin-gold nanoformulation: synthesis, characterizations and biomedical application, *Food Biosci.* (2023) 103446.

- [27] B. Zheng, D.J. McClements, Formulation of more efficacious curcumin delivery systems using colloid science: enhanced solubility, stability, and bioavailability, *Molecules* 25 (12) (2020) 2791.
- [28] C.I.D. Pereira, et al., Concise behavior of Curcumin in water-ethanol: critical Water Aggregation Percentage and multivariate analysis of protolytic equilibria, *Dyes Pigments* 197 (2022) 109887.
- [29] S. Rathore, et al., Curcumin: a review for health benefits, *Int. J. Res. Rev* 7 (1) (2020) 273–290.
- [30] B.B. Aggarwal, Y.-J. Surh, S. Shishodia, *The Molecular Targets and Therapeutic Uses of Curcumin in Health and Disease*, vol.595, Springer Science & Business Media, 2007.
- [31] A. Mohammadi, et al., Synthesis of curcumin loaded single walled carbon nanotubes: characterization and anticancer effects in vitro, *Results in Chemistry* (2024) 101370.
- [32] Haydar Goksu, Kemal Cellat, Fatih Şen, Single-walled carbon nanotube supported PtNi nanoparticles (PtNi@SWCNT) catalyzed oxidation of benzyl alcohols to the benzaldehyde derivatives in oxygen atmosphere, *Sci. Rep.* 10 (10) (2020) 9656, <https://doi.org/10.1038/s41598-020-66492-x>.
- [33] X. Li, et al., Formation of gold nanostar-coated hollow mesoporous silica for tumor multimodality imaging and photothermal therapy, *ACS Appl. Mater. Interfaces* 9 (7) (2017) 5817–5827.
- [34] Y.-W. Jiang, et al., Copper oxide nanoparticles induce enhanced radiosensitizing effect via destructive autophagy, *ACS Biomater. Sci. Eng.* 5 (3) (2019) 1569–1579.
- [35] M. Izci, et al., The use of alternative strategies for enhanced nanoparticle delivery to solid tumors, *Chem. Rev.* 121 (3) (2021) 1746–1803.
- [36] S. Goel, D. Ni, W. Cai, Harnessing the power of nanotechnology for enhanced radiation therapy, *ACS Nano* 11 (6) (2017) 5233–5237.
- [37] E.P. Stater, et al., The ancillary effects of nanoparticles and their implications for nanomedicine, *Nat. Nanotechnol.* 16 (11) (2021) 1180–1194.
- [38] A. De, R. Adhikary, J. Datta, Proactive role of carbon nanotube-polyaniline conjugate support for Pt nano-particles toward electro-catalysis of ethanol in fuel cell, *Int. J. Hydrogen Energy* 42 (40) (2017) 25316–25325.
- [39] S. Rele, et al., Curcumin coating: a novel solution to mitigate inherent carbon nanotube toxicity, *J. Mater. Sci. Mater. Med.* 35 (1) (2024) 24.
- [40] A. Abed, et al., Platinum nanoparticles in biomedicine: preparation, anti-cancer activity, and drug delivery vehicles, *Front. Pharmacol.* 13 (2022) 797804.
- [41] Y. Luo, et al., Targeted nanoparticles for enhanced X-ray radiation killing of multidrug-resistant bacteria, *Nanoscale* 5 (2) (2013) 687–694.